# Atomic mass, Bjorken variable, and scale dependence of quark transport coefficient in Drell-Yan process for proton incident on nucleus*

Wei-Jie Xu (许卫杰)[1†] Tian-Xing Bai (白天星)[2] Chun-Gui Duan (段春贵)[1‡]

[1]College of Physics and Hebei Advanced Thin Film Laboratory, Hebei Normal University, Shijiazhuang 050024, China
[2]Hebei University of Environmental Engineering, Qinhuangdao 066102, China

**Abstract:** By means of the nuclear parton distributions determined without the fixed-target Drell-Yan experimental data and the analytic expression of quenching weight based on the BDMPS formalism, next-to-leading order analyses were performed on the Drell-Yan differential cross section ratios from the Fermilab E906 and E866 collaborations. It was found that the results calculated only with the nuclear effects of the parton distribution were not in agreement with the E866 and E906 experimental data. The incoming parton energy loss effect cannot be ignored in the nuclear Drell-Yan reactions. The predicted results indicate that, with the quark transport coefficient as a constant, the suppression due to the target nuclear geometry effect is approximately 16.85 % for the quark transport coefficient. It was shown that we should consider the target nuclear geometry effect in studying the Drell-Yan reaction on nuclear targets. On the basis of the Bjorken variable and scale dependence of the quark transport coefficient, the atomic mass dependence was incorporated. The quark transport coefficient was determined as a function of the atomic mass, Bjorken variable $x_2$, and scale $Q^2$ by the global fit of the experimental data. The determined constant factor $\hat{q}_0$ of the quark transport coefficient is $0.062 \pm 0.006$ GeV$^2$/fm. It was found that the atomic mass dependence has a significant impact on the constant factor $\hat{q}_0$ in the quark transport coefficient in cold nuclear matter.

**Keywords:** quark transport coefficient, Drell-Yan, energy loss

**DOI:** 10.1088/1674-1137/acb8a4

## I. INTRODUCTION

The insight into quark-gluon plasma (QGP) properties has been one of the most active frontiers in nuclear physics and particle physics to date. Jet quenching can provide a unique window into the nature of the QGP produced in heavy-ion collisions [1, 2]. To realize jet quenching, it is necessary to determine the energy loss mechanism theoretically because the initial scattering partons with high transverse momentum propagate through the QGP while losing energy. However, the energy loss mechanism is still not clearly known [3–9].

As for the Drell-Yan reaction [10] of hadrons on the nucleus and the semi-inclusive deep inelastic scattering of leptons on the nucleus, the bound nucleons in the target nucleus play the role of very nearby detectors for the traversing partons. The hard scattering is localized in space. The properties of the target nuclei are well known. In addition, the semi-inclusive deep inelastic scattering on nuclear targets is an ideal tool to study the energy loss of the outgoing parton in the cold nuclear medium [11–15]. The hadron-induced Drell-Yan reaction on nuclear targets is an excellent process to investigate the incoming parton energy loss in cold nuclear matter [16–23]. Therefore, the Drell-Yan reaction of hadrons on the nucleus and the semi-inclusive deep inelastic scattering of leptons on the nucleus can provide the essential information on the energy loss mechanism of fast partons in cold nuclear matter, which helps to explore the similar process appearing in relativistic heavy ion collisions.

According to the parton model interpretation, the Drell-Yan process in hadron-nucleus collisions is closely related to the parton distribution functions in nuclei. It is well known that the nuclear parton distribution functions are mutually different from those in free nucleons [24, 25]. The nuclear modifications to the nucleon parton distribution functions are usually referred to as the nuclear effects on the parton distribution functions. In considera-

Received 25 October 2022; Accepted 31 January 2023; Published online 1 February 2023
* Supported in part by the National Natural Science Foundation of China (11975090, 11575052).
† E-mail: wjxu@hebtu.edu.cn
‡ E-mail: duancg@hebtu.edu.cn(Corresponding author)
Content from this work may be used under the terms of the Creative Commons Attribution 3.0 licence. Any further distribution of this work must maintain attribution to the author(s) and the title of the work, journal citation and DOI. Article funded by SCOAP[3] and published under licence by Chinese Physical Society and the Institute of High Energy Physics of the Chinese Academy of Sciences and the Institute of Modern Physics of the Chinese Academy of Sciences and IOP Publishing Ltd

tion of the strong necessity of precise nuclear parton distributions, the global analysis of nuclear parton distribution functions has been employed for over 20 years [26]. Several groups have presented their global analysis of the nuclear parton distribution functions. They are Eskola *et al*. (EKS98 [27], EKPS [28], EPS09 [29], EPPS16 [30], and EPPS21 [31]), Hirai *et al*. (HKM [32], HKN04 [33], and HKN07 [34]), de Florian *et al*. (nDS [35] and DSZS [36]), I. Schienbein *et al*. [37], K. Kovarik *et al*. (nCTEQ15 [38]), Marina Walt *et al*. (TUJU19 [39]), and Rabah Abdul Khalek *et al*. (nNNPDF1.0 [40] and nNNPDF2.0 [41]). It is worth noting that HKM, TUJU19, nNNPDF1.0, and nNNPDF2.0 proposed nuclear parton distributions that did not employ the existing experimental data on the fixed-target Drell-Yan process.

As for hadron-nucleus Drell-Yan process, the energy loss of incoming partons is another nuclear effect apart from the nuclear effects on the parton distributions as in deep inelastic scattering. To investigate the energy loss of a high energy parton in the cold nuclear matter, Baier *et al*. [42–45] (BDMPS hereafter) treated the multiple scattering of the high energy quark in the nucleus by the Glauber approximation. The medium-induced transverse momentum broadening and induced gluon radiation spectrum of a high energy quark traversing a nucleus were studied. BDMPS showed that the radiative energy loss of the parton per unit length grows as the length of the nuclear matter increases, as does the transverse momentum broadening. In the BDMPS formalism, the quark transport coefficient not only determines the energy loss, but it is also related to the transverse momentum broadening of energetic partons propagating in the medium. The quark transport coefficient is defined as

$$\hat{q} = \frac{4\pi^2\alpha_s(Q_{\rm G}^2)C_F}{N_c^2-1}\rho x_{\rm G} G(x_{\rm G}, Q_{\rm G}^2), \tag{1}$$

where $C_F$ is the quark colour factor, the number of colors $N_c = 3$, and $\rho$ is the nuclear matter density. The strong coupling constant $\alpha_s$ and the gluon distribution function $G(x_{\rm G}, Q_{\rm G}^2)$ depend on the $Q_{\rm G}^2$ virtuality. The theoretical calculation from BDMPS indicates that the Bjorken variable $x_{\rm G} \ll 1$ (see Appendix B in Ref. [42]). The $Q_{\rm G}^2$ virtuality is equal to the transverse momentum broadening of energetic partons. The experimental data from the CERN experiment NA10 [46] and Fermilab experiment E772 [47] show that the $Q_{\rm G}^2$ virtuality is less than 1 GeV$^2$. However, it is important to keep in mind that the Bjorken variable $x_{\rm G}$ estimated in theory is an unmeasurable kinematic variable in an experiment. This fact limits the predictive power of the BDMPS theory.

To improve the predictive power of theory, we explored the relation between the quark transport coefficient and the measurable kinematic variable in deep inelastic scattering [15] and the nuclear Drell-Yan reaction [22].

By means of the semi-inclusive deep inelastic scattering of leptons on the nucleus, we used the analytic parameterization of quenching weight based on the BDMPS formalism [48] with the target nuclear geometry effect. The hadron multiplicity ratios were calculated by comparison to the HERMES charged pions production data [49] on the quark hadronization occurring outside the nucleus. A relation was discovered between the quark transport coefficient and the measurable kinematic variables in deep inelastic scattering. The quark transport coefficient was determined as a function of the Bjorken variable and photon virtuality [15].

By means of the proton-nucleus Drell-Yan process, we used the HKM nuclear parton distributions [32] determined only with lepton-nuclear deep inelastic scattering experimental data and the analytic parameterization of quenching weight based on the BDMPS formalism. The nuclear Drell-Yan differential cross section ratios were computed as a function of the Feynman variable from Fermilab E906 [50] and E866 [51] experimental data. A relation was discovered between the quark transport coefficient and the measurable kinematic variables in the Drell-Yan process. The quark transport coefficient was determined as a function of the invariant mass of the lepton pair and the momentum fraction of the partons in the target nucleus [22].

In the two published papers [15, 22], our theoretical calculations were performed at the leading order QCD approximation. The atomic mass dependence was not involved in the quark transport coefficient.

In fact, a high energy parton encounters various nucleons in the target nucleus when it traverses cold nuclear matter. In the definition of quark transport coefficient, the gluon distribution function $G(x_{\rm G}, Q_{\rm G}^2)$ should be that of the bound nucleon in the target nucleus. In other words, the gluon distribution function $G(x_{\rm G}, Q_{\rm G}^2)$ depends on the atomic mass number. In the present article, a next-to-leading order analysis of the differential cross section ratios in the nuclear Drell-Yan process from Fermilab E906 [50] and E866 [51] experimental data is performed. The nuclear effects on the parton distribution functions, energy loss effect based on the BDMPS formalism, and target nuclear geometry effect are discussed respectively. The atomic mass, Bjorken variable, and scale dependence of the quark transport coefficient are explored for the first time. It is expected that new knowledge will be gained about the quark transport coefficient in the cold nuclear medium.

The remainder of the paper is organized as follows. In Sec. II, the brief formalism for the differential cross section in the nuclear Drell-Yan process is presented. In Sec. III, the results and discussion obtained are presented. Finally, a summary is presented.

## II. BRIEF FORMALISM FOR DIFFERENTIAL CROSS SECTION IN NUCLEAR DRELL-YAN REACTION

As for proton-nucleus Drell-Yan process [10], the perturbative QCD leading order contribution is quark-antiquark annihilation into a lepton pair of mass $M$. In the collinear factorization approach, which is valid in the current study [52, 53], the leading order (LO) Drell-Yan cross section in Feynman variable $x_{\rm F}$ and $M$ is given by

$$\frac{{\rm d}^2\sigma^{\rm LO}}{{\rm d}M{\rm d}x_{\rm F}} = \frac{8\pi\alpha_{\rm em}^2}{9Ms}\frac{1}{x_1+x_2}H^{\rm LO}(x_1,x_2,Q^2), \tag{2}$$

with

$$H^{\rm LO}(x_1,x_2,Q^2) = \sum_f e_f^2[q_f^p(x_1,Q^2)\bar{q}_f^A(x_2,Q^2) + \bar{q}_f^p(x_1,Q^2)q_f^A(x_2,Q^2)], \tag{3}$$

where $\alpha_{\rm em}$ is the fine structure coupling constant, $\sqrt{s}$ is the center of mass energy of the hadronic collision, $x_1$ (respectively $x_2$) is the momentum fraction carried by the projectile (respectively target) parton, the factorization scale $Q^2 = M^2$, the sum is carried out over the light flavor $f = u$, $d$, $s$, and $q_f^{p(A)}(x,Q^2)$ and $\bar{q}_f^{p(A)}(x,Q^2)$ are the quark and antiquark distributions in the proton (nucleon in the nucleus $A$).

In the perturbative QCD next-to-leading order (NLO) approximation, additional emission of a parton (quark or gluon) into the final state has to be taken into account. The NLO contribution includes quark-antiquark annihilation processes $(q+\bar{q}\to\gamma^*+g)$ and gluon Compton scattering $(q+g\to\gamma^*+q)$. The NLO correction to the Drell-Yan cross section is given by

$$\frac{{\rm d}^2\sigma^{\rm NLO}}{{\rm d}M{\rm d}x_{\rm F}} = \frac{8\pi\alpha_{\rm em}^2}{9Ms}\frac{\alpha_s(M^2)}{2\pi}\int_0^1 {\rm d}z\frac{1}{x_1+x_2}H^{\rm NLO}(x_1,x_2,Q^2,z), \tag{4}$$

with

$$H^{\rm NLO}(x_1,x_2,Q^2,z) = \sum_f e_f^2\{q_f^p(x_1,Q^2)\bar{q}_f^A(x_2,Q^2)f_q(z) + g^p(x_1,Q^2)[q_f^A(x_2,Q^2) + \bar{q}_f^A(x_2,Q^2)]f_g(z) + (x_1\leftrightarrow x_2)\}, \tag{5}$$

where $g^{p(A)}(x,Q^2)$ are the gluon distributions in the proton (nucleon in the nucleus $A$). By combining the dimensionless variable $\tau = zx_1x_2$ and the Feynman variable $x_{\rm F} = x_1 - x_2$, one can easily find that

$$x_1 = \frac{1}{2}(\sqrt{x_{\rm F}^2+4(\tau/z)}+x_{\rm F}), \quad x_2 = \frac{1}{2}(\sqrt{x_{\rm F}^2+4(\tau/z)}-x_{\rm F}). \tag{6}$$

The coefficient functions $f_{q,g}(z)$ [54, 55] are, in the $\overline{\rm MS}$ factorization scheme,

$$\begin{aligned} f_q(z) =& C_F\left\{4(1+z^2)\left(\frac{\ln(1-z)}{1-z}\right)_+ - 2\frac{1+z^2}{1-z}\ln z + \delta(1-z)\left(\frac{2\pi^2}{3}-8\right)\right\},\\ f_g(z) =& T_R\left\{(z^2+(1-z)^2)\ln\frac{(1-z)^2}{z}+\frac{1}{2}+3z-\frac{7}{2}z^2\right\}, \end{aligned} \tag{7}$$

with $C_F = 4/3$, $T_R = 1/2$. The "plus" distributions are defined by

$$\int_0^1 {\rm d}x f(x)[g(x)]_+ = \int_0^1 {\rm d}x(f(x)-f(1))g(x). \tag{8}$$

Therefore, up to the next to leading order, the differential cross section in a Drell-Yan reaction can be written as

$$\frac{{\rm d}^2\sigma}{{\rm d}M{\rm d}x_{\rm F}} = \frac{{\rm d}^2\sigma^{\rm LO}}{{\rm d}M{\rm d}x_{\rm F}} + \frac{{\rm d}^2\sigma^{\rm NLO}}{{\rm d}M{\rm d}x_{\rm F}}. \tag{9}$$

In the hadron-nucleus Drell-Yan reaction, the projectile suffers multiple collisions and repeated energy losses in the nuclear matter. In other words, each quark or gluon in the beam hadron can lose a finite fraction of its energy in the nuclear target owing to QCD bremsstrahlung. After considering the parton energy loss in nuclei, the incident parton momentum fraction can be shifted from $x_1+\Delta x_1$ to $x_1$ at the point of fusion. $\Delta x_1 = \Delta E/E_p$ with $\Delta E$ ($E_p$) being the quark energy loss in the nuclear medium (the projectile hadron energy). After adding the energy loss of the incoming parton in the target nucleus,

$$\begin{aligned} H^{\rm LO}(x_1,x_2,Q^2) =& \int_0^{(1-x_1)E_p}{\rm d}(\Delta E)P_q(\Delta E,\omega_c,L)H^{\rm LO} \times(x_1+\Delta x_1,x_2,Q^2),\\ H^{\rm NLO}(x_1,x_2,Q^2,z) =& \int_0^{(1-x_1)E_p}{\rm d}(\Delta E)\sum_f e_f^2\{P_q(\Delta E,\omega_c,L) \times q_f^p(x_1+\Delta x_1,Q^2)\bar{q}_f^A(x_2,Q^2)f_q(z) + P_g(\Delta E,\omega_c,L)g^p(x_1+\Delta x_1,Q^2) \times[q_f^A(x_2,Q^2)+\bar{q}_f^A(x_2,Q^2)]f_g(z) + (x_1\leftrightarrow x_2)\}, \end{aligned} \tag{10}$$

where the quenching weights $P_{q,g}(\Delta E,\omega_c,L)$ are the prob-

ability that the radiated gluons carry altogether a given energy $\Delta E$ for an incident quark and gluon, respectively. $\omega_c$ is the characteristic gluon frequency, which is equal to $(1/2)\hat{q}L^2$ with the path length $L$ traversed by the incoming parton.

If we do not consider the target nuclear geometry effect, the average path length of the incident parton in the nucleus is given by $L=(3/4)R_A$ for the case of a hard-sphere nucleus. The nuclear radius $R_A=1.12A^{1/3}$ fm with atomic mass number $A$ [56]. By adding the target nuclear geometry effect [14], the colored incoming parton interacting at the coordinate $y$ along the direction of the incident quark will traverse the path length $L=\sqrt{R_A^2-b^2}+y$, with $\vec{b}$ being its impact parameter. After taking both nuclear geometry and energy loss effects into account,

$$\begin{aligned}
H^{\rm LO}(x_1,x_2,Q^2) &= \int {\rm d}^2b{\rm d}y\rho_A(\vec{b},y)\int_0^{(1-x_1)E_p}{\rm d}(\Delta E)\\
&\times P_q(\Delta E,\omega_c,L)H^{\rm LO}(x_1+\Delta x_1,x_2,Q^2),\\
H^{\rm NLO}(x_1,x_2,Q^2,z) &= \int {\rm d}^2b{\rm d}y\rho_A(\vec{b},y)\int_0^{(1-x_1)E_p}{\rm d}(\Delta E)\\
&\times\sum_f e_f^2\{P_q(\Delta E,\omega_c,L)\\
&\times q_f^p(x_1+\Delta x_1,Q^2)\bar{q}_f^A(x_2,Q^2)f_q(z)\\
&+P_g(\Delta E,\omega_c,L)g^p(x_1+\Delta x_1,Q^2)\\
&\times[q_f^A(x_2,Q^2)+\bar{q}_f^A(x_2,Q^2)]f_g(z)\\
&+(x_1\leftrightarrow x_2)\},
\end{aligned}\tag{11}$$

where $\rho_A(\sqrt{b^2+y^2})=(\rho_0/A)\Theta(R_A-\sqrt{b^2+y^2})$ with $\rho_0$ being the nuclear density.

## III. RESULTS AND DISCUSSION

In the present analysis, the experimental data are taken from the E906 [50] and E866 [51] collaborations at Fermilab. The E866 Collaboration reported the observation of the ratios of the Drell-Yan cross section per nucleon for an 800 GeV proton beam incident on Be (beryllium), Fe (iron), and W (tungsten) targets. The Drell-Yan events were recorded in the range $4.0<M<8.4$ GeV, $0.01<x_2<0.12$, $0.21<x_1<0.95$, and $0.13<x_{\rm F}<0.93$. The E906 Collaboration performed the observation of the ratios of the Drell-Yan cross section per nucleon for an 120 GeV proton beam incident on C (carbon), Fe, and W targets. Muon pairs were recorded in the ranges $4.5<M<5.5$ GeV and $0.1<x_2<0.3$. To emphasize, the E866 and E906 data cover the momentum fraction of the target parton from 0.01 to 0.12, and from 0.1 to 0.3, respectively. Because of this, the E866 and E906 data possibly show the measurable kinematic variables dependence of the quark transport coefficient in the cold nuclear medium.

To study the property of the quark transport coefficient, we calculate the Drell-Yan cross section ratio of two different nuclear targets bombarded by a proton,

$$R_{A_1/A_2}(x_{\rm F})=\int\frac{{\rm d}^2\sigma^{pA_1}}{{\rm d}M{\rm d}x_{\rm F}}{\rm d}M\Big/\int\frac{{\rm d}^2\sigma^{pA_2}}{{\rm d}M{\rm d}x_{\rm F}}{\rm d}M,\tag{12}$$

in perturbative QCD next-to-leading order approximation. The comparison is performed with selected experimental data. The integral range in the above equation is given by means of the relative experimental kinematic region.

To research the nuclear effects from parton distribution functions on the Drell-Yan differential cross section ratio, $\chi^2$ is calculated with the Drell-Yan differential cross section rations $R_{A_1/A_2}$ as

$$\chi^2=\sum_j\frac{(R^{\rm data}_{A_1/A_2,j}-R^{\rm theo}_{A_1/A_2,j})^2}{(R^{\rm err}_{A_1/A_2,j})^2},\tag{13}$$

where the experimental error is given by $R^{\rm err}_{A_1/A_2,j}$, and $R^{\rm data}_{A_1/A_2,j}(R^{\rm theo}_{A_1/A_2,j})$ indicates the experimental data (theoretical) value for the Drell-Yan differential cross section ratio $R_{A_1/A_2}$ as a function of the Feynman variable. We employ the nNNPDF2.0 nuclear parton distribution functions from the NNPDF collaboration [41] in our calculations without considering the quark energy loss effect. The calculated values of $\chi^2$ per degrees of freedom are 0.511, 3.071, 6.899, and 7.259 for the Drell-Yan differential cross section ratios Fe/Be, W/Be, Fe/C, and W/C, respectively. Our obtained values of $\chi^2$/ndf are 1.791 and 7.079 for the E866 and E906 experimental data, respectively. In total, the value of $\chi^2$/ndf is given by 4.057 for the E906 and E866 experimental data (see Table 1). The theoretical results in the global fit are compared with the measured Drell-Yan differential cross-section ratios from the E906 and E866 collaborations in Fig. 1 (black solid curves). Obviously, the calculated results where only the nuclear effects of parton distribution are considered do not agree with the E866 and E906 experimental data. In addition, the main contribution of $\chi^2$/ndf is from the E906 experimental data in the global fit. It is found that the value of $\chi^2$/ndf from the cross-section ratio Fe/Be is remarkably lower than those from W/Be, Fe/C, and W/C. It is shown that the theoretical prediction is in good agreement with the experimental data on the cross section ratio Fe/Be. We consider that the theoretical result overestimates the nuclear effects on parton distribution functions in the Drell-Yan differential cross section ratio Fe/Be. Therefore, it is necessary to refine the nuclear parton distribution in the future. The accurate nuclear parton

**Table 1.** Values of $\hat{q}_0$ and $\chi^2$/ndf extracted from fitting the selected experimental data on the Drell-Yan differential cross section ratio from the E906 and E866 experiments by considering the nuclear effects on the parton distribution functions (NEPDF) and adding the energy loss (EL) effect without and with the nuclear geometry effect.

| | E866 | | E906 | |
|---|---|---|---|---|
| | Fe/Be | W/Be | Fe/C | W/C |
| NEPDF | $\chi^2$/ndf = 0.511 | $\chi^2$/ndf = 3.071 | $\chi^2$/ndf = 6.899 | $\chi^2$/ndf = 7.259 |
| | $\chi^2$/ndf = 1.791 | | $\chi^2$/ndf = 7.079 | |
| | $\chi^2$/ndf = 4.057 | | | |
| EL ($L = 3/4R_A$) | $\hat{q}_0 = 0$ | $\hat{q}_0 = 0.858 \pm 0.211$ | $\hat{q}_0 = 0.739 \pm 0.074$ | $\hat{q}_0 = 0.336 \pm 0.030$ |
| | $\chi^2$/ndf = 0.511 | $\chi^2$/ndf = 0.546 | $\chi^2$/ndf = 1.102 | $\chi^2$/ndf = 0.413 |
| | $\hat{q}_0 = 0.873 \pm 0.198$ | | $\hat{q}_0 = 0.363 \pm 0.017$ | |
| | $\chi^2$/ndf = 0.667 | | $\chi^2$/ndf = 2.013 | |
| | $\hat{q}_0 = 0.362 \pm 0.034$ $\chi^2$/ndf = 1.345 | | | |
| EL($L = \sqrt{R_A^2 - b^2} + y$) | $\hat{q}_0 = 0.301 \pm 0.005$ $\chi^2$/ndf = 0.879 | | | |

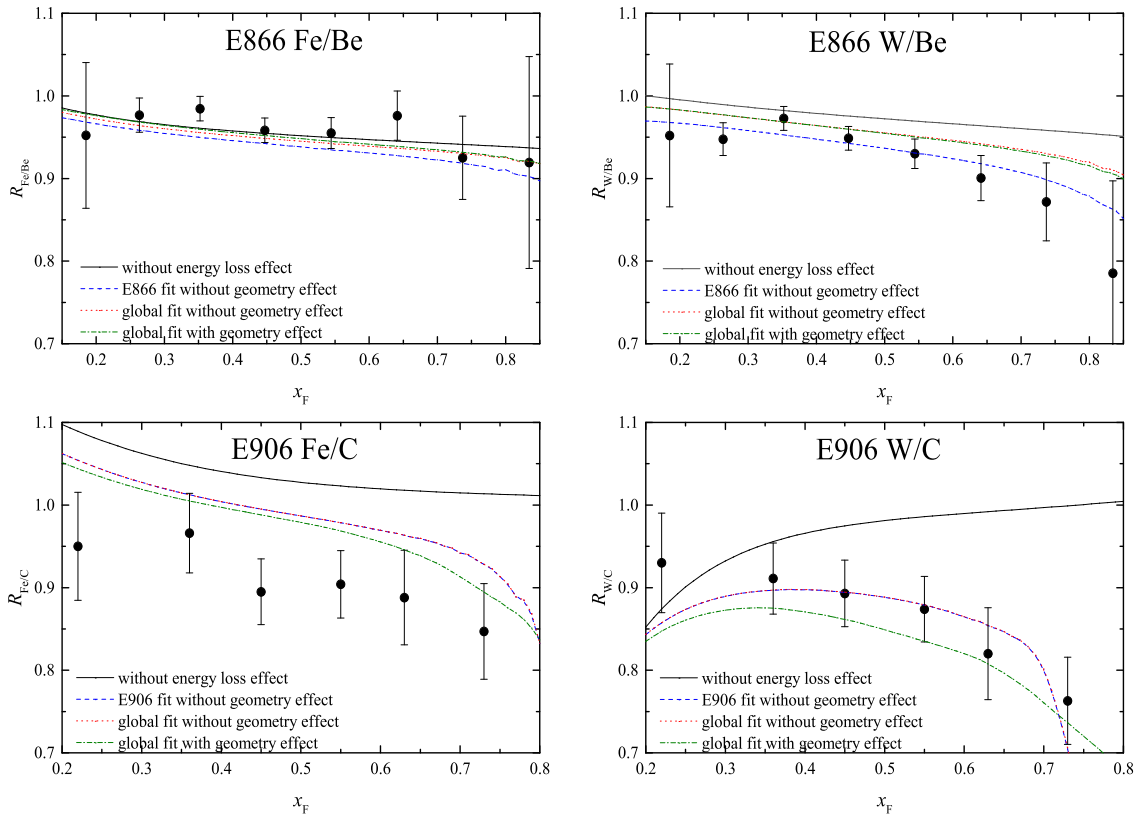


**Fig. 1.** (color online) Ratios of the differential cross section per nucleon for the Drell-Yan reaction versus Feynman variable $x_F$. The black solid curves are the predicted cross-section ratios in the global fitting of the E906 and E866 experimental data without the energy loss effect. The blue dashed curves are the predicted results from fitting the E906 and E866 data, respectively, without the target nuclear geometry effect. As for the global fitting of E906 and E866 measurements, the red dotted (green dot-dashed) curves correspond to the theoretical predictions without (with) the target nuclear geometry effect. The experimental data are taken from the E906 and E866 collaborations.

distribution can highlight the potential of the fixed-target Drell-Yan measurements to probe the parton energy loss mechanism in a robust manner.

On the basis of the nuclear effects on parton distribution functions, the energy loss effect of the incoming parton is added in the following. The analytic expressions

$P(\Delta E, \omega_c, L)$ [48] for the quark and gluon quenching weight can be given by using the BDMPS gluon radiation spectrum for an incoming parton in QCD media [57],

$$\omega_c P(\bar{\Delta E} = \frac{\Delta E}{\omega_c}) = \frac{1}{\sqrt{2\pi}\sigma\bar{\Delta E}} \exp\left[-\frac{(\log\bar{\Delta E} - \mu)^2}{2\sigma^2}\right], \quad (14)$$

with parameters $(\mu, \sigma) = (-2.55, 0.57)$ and $(\mu, \sigma) = (-1.54, 0.38)$ for the incoming quark and gluon, respectively. The simple analytic expressions can easily be used to compute the Drell-Yan differential cross section. By means of the CERN subroutine MINUIT [58], the undetermined parameters in the quark transport coefficient $\hat{q}$ can be obtained by minimizing $\chi^2$.

We first make the quark transport coefficient $\hat{q}$ as a constant $\hat{q}_0$ without its kinematic variable dependence. If we neglect the target nuclear geometry effect, the incoming hard parton will travel an average path length $L = (3/4)R_A$ in the target nuclear medium. Consequently, only one parameter $\hat{q}_0$ needs to be pinned down. The values of $\hat{q}_0$ and $\chi^2$/ndf extracted from fitting the selected experimental data on the Drell-Yan differential cross section ratio are listed in Table 1. The calculated values of $\hat{q}_0$ ($\chi^2$/ndf) are 0.0 GeV$^2$/fm (0.511), $0.858 \pm 0.211$ GeV$^2$/fm (0.546), $0.739 \pm 0.074$ GeV$^2$/fm (1.102), and $0.336 \pm 0.030$ GeV$^2$/fm (0.413) for the Drell-Yan differential cross section ratios Fe/Be, W/Be, Fe/C, and W/C, respectively. The obtained values of $\hat{q}_0$ ($\chi^2$/ndf) are $0.873 \pm 0.198$ GeV$^2$/fm (0.667) and $0.363 \pm 0.017$ GeV$^2$/fm (2.013) for the E866 and E906 experimental data, respectively. In view of the different $x_2$ ranges measured in the E906 and E866 experiments, we can obviously conclude that the quark transport coefficient $\hat{q}$ depends on the momentum fraction of the target parton. However, it is unfortunate that the global fitting the E906 and E866 experimental data gives $\hat{q}_0 = 0.362 \pm 0.034$ GeV$^2$/fm with $\chi^2$/ndf = 1.345. Therefore, it is worth intensively looking into the kinematic variable dependence of the quark transport coefficient. Just to confirm this conclusion, we will need to have higher-precision (large-statistics) data on the Drell-Yan differential cross section ratio. We are very hopeful that such new results will be obtained from the Fermilab 906 and 866 collaborations.

To demonstrate intuitively the energy loss effect of an incoming parton on the Drell-Yan cross section ratio, the calculated results combining nNNPDF2.0 nuclear parton distribution functions are compared with the selected experimental data in Fig. 1. The blue dashed curves indicate the predicted cross-section ratios for the case of fitting the E906 and E866 data without the target nuclear geometry effect. As for the global fitting of E906 and E866 measurements, the red dotted curves indicate the theoretical predictions without the target nuclear geometry effect. In particular, it is worth mentioning the Drell-Yan cross section ratio of Fe and C nuclear targets bombarded by a proton. As presented in Table 1 and Fig. 1, the agreement is not consistent between the experimental data and the theoretical results from fitting the E906 measurement and only the cross section ratio Fe/C. This fact reminds us that the precise measurement of the ratios of the Drell-Yan cross section per nucleon and accurate nuclear parton distribution functions are indispensable for a deep understanding of the energy loss mechanism in the cold nuclear medium.

Furthermore, we explore the energy loss with the target nuclear geometry effect on the Drell-Yan cross section ratio. In this case, the path length $L = \sqrt{R_A^2 - b^2} + y$ for the incident parton traversing the nucleus. Our calculated result indicates that $\hat{q}_0 = 0.301 \pm 0.005$ GeV$^2$/fm with $\chi^2$/ndf = 0.879 from the global fitting of the E906 and E866 experimental data. A comparison of our theoretical expectations (green dot-dashed curves) is presented with the experimental measurements in Fig. 1. From Table 1, it is found that the target nuclear geometry effect could reduce the central value of the quark transport coefficient $\hat{q}_0$ by as much as 16.85 %. Therefore, we should consider the target nuclear geometry effect over the course of studying the nuclear Drell-Yan reaction.

Now, let us investigate the kinematic variable dependence of the quark transport coefficient. In our preceding article [22], we discovered the relation between the Bjorken variable $x_G$ in the quark transport coefficient and the momentum fraction of the target parton in the Drell-Yan process. In other words, the Bjorken variable $x_G$ can be replaced with the momentum fraction $x_2$. Consequently, we can deduce that the virtuality $Q_G^2$ should also be expressed with the measurable scale $Q^2$, which is the square of the lepton pair mass $M$. By means of fitting the experimental data on the Drell-Yan cross section ratio, the quark transport coefficient has been determined as a function of the Bjorken variable $x_2$ and scale $Q^2$.

Regarding the gluon density $x_G G(x_G, Q_G^2)$ from the quark transport coefficient $\hat{q}$, $x_G \ll 1$ and $Q_G^2 < 1$ GeV$^2$ [22]. A phenomenological work [59] provided a model based on the concept of saturation for small $Q_G^2$ and small $x_G$. A good description of data on the proton structure function was presented by means of the proton saturation scale. According to the saturation model, the gluon density

$$x_G G(x_G, Q_G^2) \sim x_G^{-\lambda}. \quad (15)$$

Using the Bjorken variable $x_2$ instead of $x_G$,

$$x_G G(x_G, Q_G^2) \sim x_2^{-\lambda}. \quad (16)$$

Hence, the Bjorken variable $x_2$ dependence of the quark

transport coefficient can be written as

$$\hat{q} = \hat{q}_0 x_2^{\alpha}. \tag{17}$$

Furthermore, adding the intermediate and large $x_2$ correction with the evolution of gluon distribution with $Q^2$, the quark transport coefficient can be supposed to be

$$\hat{q}(x_2, Q^2) = \hat{q}_0 \alpha_s(Q^2) x_2^{\alpha} (1-x_2)^{\beta} \ln^{\gamma}(Q^2/Q_0^2), \tag{18}$$

where $Q_0^2 = 1$ GeV$^2$ to make the argument in the logarithm dimensionless. The strong coupling constant

$$\alpha_s(Q^2) = \frac{4\pi}{\left(11 - \frac{2N_f}{3}\right)\ln\left(\frac{Q^2}{\Lambda_{\rm QCD}^2}\right)} \tag{19}$$

for $N_f = 3$ at leading order [60], with $\Lambda_{\rm QCD} = 0.2$ GeV. The four undetermined parameters are $\hat{q}_0$, $\alpha$, $\beta$, and $\gamma$.

In fact, the gluon density $x_{\rm G}G(x_{\rm G}, Q_{\rm G}^2)$ in the quark transport coefficient should be that of the bound nucleon in the target nucleus. The gluon density $x_{\rm G}G(x_{\rm G}, Q_{\rm G}^2)$ depends on the atomic mass number in the fixed-target experiment. The saturation scale of a nucleus [61, 62] is enhanced relative to the nucleon one by a factor $A^{1/3}$. With the atomic mass number $A$ and $x_2$ dependence of the saturation scale in the nucleus, the gluon density

$$x_{\rm G}G(x_{\rm G}, Q_{\rm G}^2) \sim A^{1/3} x_{\rm G}^{-\lambda} \sim A^{1/3} x_2^{-\lambda}. \tag{20}$$

Therefore, we can give the atomic mass, Bjorken variable, and scale dependence of the quark transport coefficient,

$$\hat{q}(A, x_2, Q^2) = \hat{q}_0 A^{1/3} \alpha_s(Q^2) x_2^{\alpha} (1-x_2)^{\beta} \ln^{\gamma}(Q^2/Q_0^2). \tag{21}$$

Thus, there are still four parameters to fit: $\hat{q}_0$, $\alpha$, $\beta$, and $\gamma$.

We perform the global analysis of the quark transport coefficient by comparing with the experimental data from the E906 and E866 collaborations. The parameter values are pinned down in the quark transport coefficient.

As for the quark transport coefficient with and without atomic mass dependence, a comparison of our theoretical results is presented with the experimental data in Fig. 2. The extracted parameter values are summarized in Table 2. It is shown that the atomic mass dependence

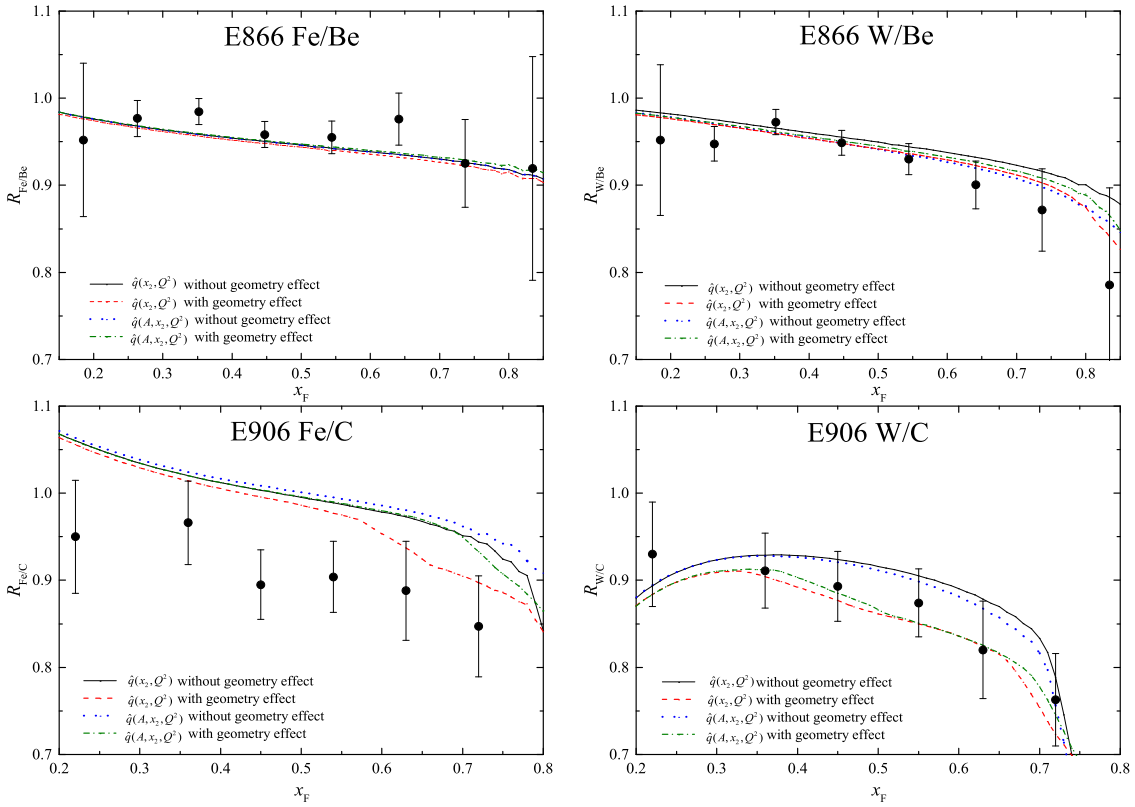


**Fig. 2.** (color online) Calculated Drell-Yan cross section ratios $R_{A/B}$ versus Feynman variable $x_{\rm F}$. The black solid (red dashed) curves are the predicted cross-section ratios from the quark transport coefficient $\hat{q}(x_2, Q^2)$ without (with) the target nuclear geometry effect. The blue dotted (green dot-dashed) curves correspond to the theoretical predictions for the quark transport coefficient $\hat{q}(A, x_2, Q^2)$ without (with) the target nuclear geometry effect. The experimental data are taken from the E906 and E866 collaborations.

**Table 2.** Parameter values of $\hat{q}$ and $\chi^2$/ndf extracted by the global analysis of E866 and E906 experimental data.

| $\hat{q}$(GeV$^2$/fm) | $\hat{q}_0$ | $\alpha$ | $\beta$ | $\gamma$ | $\chi^2$/ndf |
|---|---|---|---|---|---|
| $\hat{q}(x_2, Q^2)$ (without geometry effect) | $0.367 \pm 0.021$ | $-0.082 \pm 0.028$ | $3.942 \pm 0.413$ | $1.570 \pm 0.051$ | 1.624 |
| $\hat{q}(x_2, Q^2)$ (with geometry effect) | $0.446 \pm 0.023$ | $-0.090 \pm 0.046$ | $3.991 \pm 0.032$ | $1.395 \pm 0.023$ | 1.095 |
| $\hat{q}(A, x_2, Q^2)$ (without geometry effect) | $0.050 \pm 0.004$ | $-0.240 \pm 0.039$ | $4.217 \pm 0.421$ | $1.554 \pm 0.077$ | 1.478 |
| $\hat{q}(A, x_2, Q^2)$ (with geometry effect) | $0.062 \pm 0.006$ | $-0.080 \pm 0.012$ | $3.671 \pm 0.023$ | $1.442 \pm 0.032$ | 1.073 |

reduces the central value of the constant factor $\hat{q}_0$ in the quark transport coefficient by approximately 86.4 % without the target nuclear geometry effect. After incorporating the target nuclear geometry effect, the atomic mass dependence reduces the central value of the constant factor $\hat{q}_0$ in the quark transport coefficient by as much as 86.1 %. Therefore, the atomic mass dependence has a significant impact on the constant factor $\hat{q}_0$ in the quark transport coefficient in cold nuclear matter.

Two other research groups have explored the transport coefficient in cold nuclear matter. François Arleo *et al*. [21, 63] studied the transport coefficient parameterization as a function of the Bjorken variable without the $Q^2$ virtuality evolution. The coefficient $\hat{q}_0$ is the only parameter of their model. The value of $\hat{q}_0$ is given by $0.07 - 0.09$ GeV$^2$/fm. In their calculation of the nuclear Drell-Yan production ratios, the EPPS16 nuclear parton distributions [30] were used. It is considered that the energy loss effect is underestimated in their phenomenological results because the Drell-Yan data sets are included in the global analysis of the EPPS16. Peng Ru *et al*. [64] performed the global analysis of the jet transport coefficient in the framework of the generalized QCD factorization formalism. The jet transport coefficient has the Bjorken-$x$ and scale $Q^2$ dependent parametrization. The coefficient $\hat{q}_0$ is $0.0195^{+0.0085}_{-0.0065}$GeV$^2$/fm. Therefore, it is expected that theoretical progress will be made in the future. With the precision experimental data on the semi-inclusive deep-inelastic scattering and nuclear Drell-Yan reaction, a quantitative understanding of the parton energy loss mechanism will be thus achieved in cold nuclear matter.

## IV. CONCLUDING REMARKS

We studied the Drell-Yan process in proton-nucleus collisions, supplementing the perturbative QCD factorized formalism with radiative parton energy loss. By means of the nuclear parton distributions determined without the fixed-target Drell-Yan process experimental data and the analytic expression of quenching weight based on the BDMPS formalism, next-to-leading order analyses on the differential cross section ratios from the nuclear Drell-Yan process were performed and compared with the experimental data from the Fermilab E906 and E866 collaborations. It was found that the results calculated only considering the nuclear effects of parton distribution do not agree with the E866 and E906 experimental data. The incoming quark energy loss effect is indispensable in the nuclear Drell-Yan process. With the quark transport coefficient as a constant and no target nuclear geometry effect, the global fitting of the E906 and E866 experimental data gives $\hat{q}_0 = 0.362 \pm 0.034$ GeV$^2$/fm. With the target nuclear geometry effect, $\hat{q}_0 = 0.301 \pm 0.005$ GeV$^2$/fm. The suppression due to the target nuclear geometry effect is approximately 16.85 % for the quark transport coefficient. It was shown that we should consider the nuclear geometry effect over the course of studying the Drell-Yan reaction on nuclear targets. On the basis of the Bjorken variable and scale dependence of the quark transport coefficient, the atomic mass dependence was combined. The quark transport coefficient was determined as a function of the atomic mass, Bjorken variable $x_2$, and scale $Q^2$ by the global fit of the experimental data. The values of the constant factor $\hat{q}_0$of the quark transport coefficient are$0.446 \pm 0.023$ GeV$^2$/fm and $0.062 \pm 0.006$ GeV$^2$/fm without and with the atomic mass dependence, respectively. The suppression due to atomic mass dependence is approximately 86.1 % for the constant factor $\hat{q}_0$ in the quark transport coefficient. It was found that the atomic mass dependence has a remarkable effect on the constant factor $\hat{q}_0$ in the quark transport coefficient in cold nuclear matter.

It is well known that there are a quark energy loss effect and nuclear effects on the parton distributions in the nuclear Drell-Yan process. Accurate nuclear parton distribution functions are crucial for studying deeply the energy loss mechanism in the cold nuclear medium. The proton incident nuclei Drell-Yan data can result in an overestimate for nuclear modification of the sea quark distribution function if leaving the quark energy loss effect out. Therefore, we suggest that the new global analysis of nuclear parton distribution functions should not employ the available experimental data on the fixed-target hadron-nucleus Drell-Yan process. In addition, the energy loss effect is less important in LHC p-Pb collisions at numbers of TeV [65, 66] because the parton energy loss decreases with the projectile hadron energy. Thus, the experimental data from the LHC can provide a supplement to determine the nuclear parton distribution functions [67].

The precise measurement of the ratios of the proton-

nucleus Drell-Yan cross section per nucleon is essential for clarifying the energy loss mechanism in the cold nuclear medium. We need higher-precision (large-statistics) data on the Drell-Yan differential cross section ratio. We are very hopeful that there such new results will be obtained from the Fermilab 906 and 866 collaborations.

The investigation into the energy loss mechanism in cold nuclear matter helps to understand the similar process appearing in relativistic heavy ion collisions. The hadron-induced Drell-Yan reaction on nuclei is an excellent process to explore the incoming parton energy loss in cold nuclear matter. We expect that our determined parametrization of the quark transport coefficient will provide useful information for the identification of the transport property of the quark-gluon plasma. It is desirable to operate precise measurements in the nuclear Drell-Yan process from the J-PARC [68] and LHCb-SMOG [69] experiments. These new experimental data should shed light on the parton propagation mechanism in nuclear matter.

## References


[1] J. D. Bjorken, Phys. Rev. D **27**, 140 (1983)
[2] D. d'Enterria, *Jet quenching: Datasheet from Landolt-Börnstein - Group I Elementary Particles*, Volume 23, in *Relativistic Heavy Ion Physics" in SpringerMaterials* (Springer, 2010). arXiv: 0902.2011
[3] J. Casalderrey-Solana, C. A. Salgado, Acta Phys. Polon. B **38**, 3731 (2007), arXiv:0712.3443
[4] U. A. Wiedemann, *Jet quenching in heavy ion collisions: Datasheet from Landolt-Börnstein - Group I Elementary Particles*, Volume 23, *Relativistic Heavy Ion Physics" in SpringerMaterials* (Springer, 2010), arXiv: 0908.2306
[5] A. Majumder and M. Van Leeuwen, Prog. Part. Nucl. Phys. **66**, 41 (2011), arXiv:1002.2206
[6] S. Cao and X. Wang, Rept. Prog. Phys. **84**, 024301 (2021), arXiv:2002.04028
[7] S. Cao *et al.*, Phys. Rev. C **104**, 024905 (2021), arXiv:2102.11337
[8] D. Everett *et al.*, Phys. Rev. C **103**, 054904 (2021), arXiv:2011.01430
[9] A. Kumar *et al.*, Phys. Rev. C **101**, 034908 (2020), arXiv:1909.03178
[10] S. Drell and T.M. Yan, Phys. Rev. Lett. **25**, 316 (1970)
[11] L. H. Song and C. G. Duan, Phys. Rev. C **81**, 035207 (2010), arXiv:1109.3836
[12] L. H. Song, N. Liu, and C. G. Duan, Chin. Phys. C **37**, 104102 (2013), arXiv:1310.5285
[13] L. H. Song, N. Liu, and C. G. Duan, Chin. Phys. C **37**, 084102 (2013), arXiv:1310.5692
[14] N. Liu, *et al.*, Phys. Lett. B **749**, 88 (2015), arXiv:1511.00767
[15] T. X. Bai and C. G. Duan, Eur. Phys. J. Plus **136**, 1181 (2021), arXiv:2011.14350
[16] L. H. Song, C.G. Duan, and N. Liu, Phys. Lett. **708**, 68 (2012), arXiv:1206.3815
[17] C. G. Duan *et al.*, Eur. Phys. J. C **50**, 585 (2007), arXiv:hep-ph/0609057
[18] C. G. Duan *et al.*, Eur. Phys. J. C **29**, 557 (2003), arXiv:hep-ph/0405113
[19] C. G. Duan *et al.*, Eur. Phys. J. C **39**, 179 (2005), arXiv:hep-ph/0601188
[20] C. G. Duan *et al.*, Phys. Rev. C **79**, 048201 (2009), arXiv:0811.0675
[21] F. Arleo *et al.*, JHEP **01**, 129 (2019), arXiv:1810.05120
[22] T. X. Bai and C. G. Duan, Eur. Phys. J. Plus **136**, 649 (2021), arXiv:2012.03167
[23] A. Accardi *et al.*, Riv. Nuovo. Cim. **32**, 439 (2010), arXiv:0907.3534
[24] J. J. Aubert *et al.*, Phys. Lett. B **123**, 275 (1983)
[25] J. Arrington *et al.*, Phys. Rev. C **104**, 065203 (2021), arXiv:2110.08399
[26] J. J. Ethier and E. R. Nocera, Ann. Rev. Nucl. Part. Sci. **70**, 43 (2020), arXiv:2001.07722
[27] K. J. Eskola, V. J. Kolhinen, and P. V. Ruuskanen, Nucl. Phys.B **535**, 351 (1998), arXiv:hep-ph/9802350
[28] K. J. Eskola *et al.*, JHEP **05**, 002 (2007), arXiv:hep-ph/0703104
[29] K. J. Eskola, H. Paukkunen, and C. A. Salgado, JHEP **04**, 065 (2009), arXiv:0902.4154
[30] K. J. Eskola *et al.*, Eur. Phys. J. C **77**, 163 (2017), arXiv:1612.05741
[31] K. J. Eskola et al, Eur. Phys. J. C **82**, 413 (2022)
[32] M. Hirai, S. Kumano, and M. Miyama, Phys. Rev. D **64**, 034003 (2001), arXiv:hep-ph/0103208
[33] M. Hirai, S. Kumano, and T. H. Nagai, Phys. Rev. C **70**, 044905 (2004), arXiv:hep-ph/0404093
[34] M. Hirai, S. Kumano, and T. H. Nagai, Phys. Rev. C **76**, 065207 (2007), arXiv:0709.3038
[35] D. de Florian and R. Sassot, Phys. Rev. D **69**, 074028 (2004), arXiv:hep-ph/0311227
[36] D. de Florian *et al.*, Phys. Rev. D **85**, 074028 (2012), arXiv:1112.6324
[37] I. Schienbein *et al.*, Phys. Rev. D **80**, 094004 (2009), arXiv:0907.2357
[38] K. Kovarik *et al.*, Phys. Rev. D **93**, 085037 (2016), arXiv:1509.00792
[39] M. Walt, I. Helenius, and W. Vogelsang, Phys. Rev. D **100**, 096015 (2019), arXiv:1908.03355
[40] R. A. Khalek, J. J. Ethier, and J. Rojo, Eur. Phys. J. C **79**, 471 (2019), arXiv:1904.00018
[41] R. A. Khalek *et al.*, JHEP **09**, 183 (2020), arXiv:2006.14629
[42] R. Baier *et al.*, Nucl. Phys. B **484**, 265 (1997), arXiv:hep-ph/9608322
[43] R. Baier *et al.*, Annu. Rev. Nucl. Part. Sci. **50**, 37 (2000), arXiv:hep-ph/0002198
[44] R. Baier *et al.*, Nucl. Phys. B **483**, 291 (1997), arXiv:hep-ph/9607355
[45] R. Baier *et al.*, Phys. Rev. C **58**, 1706 (1998), arXiv:hep-ph/9803473
[46] P. Bordalo *et al.*, Phys. Lett. B **193**, 373 (1987)
[47] D. M. Alde *et al.*, Phys. Rev. Lett. **66**, 2285 (1991)
[48] F. Arleo, JHEP **11**, 044 (2002), arXiv:hep-ph/0210104
[49] A. Airapetian *et al.*, Eur. Phys. J. A **47**, 113 (2011), arXiv:1107.3496
[50] P. J. Lin, *Measurement of Quark Energy Loss in Cold*

*Nuclear Matter at Fermilab E906/SeaQuest*, Ph.D. Thesis (Colorado University, 2017)
[51] M. A. Vasiliev *et al*., Phys. Rev. Lett. **83**, 2304 (1999), arXiv:hep-ex/9906010
[52] J. Qiu, arXiv: hep-ph/0305161
[53] J. Qiu and G. Sterman, Nucl. Phys. B **353**, 105 (1991)
[54] G. Altarelli, R. K. Ellis, and G. Martinelli, Nucl. Phys. B, **143**, 521 (1978), [Erratum: Nucl. Phys. B 146, 544 (1978)]
[55] G. Altarelli, R. K. Ellis, and G. Martinelli, Nucl. Phys. B **157**, 461 (1979)
[56] G. T. Garvey and J. C. Peng, Phys. Rev. Lett. **90**, 092302 (2003), arXiv:hep-ph/0208145
[57] R. Baier *et al*., Nucl. Phys. B **531**, 403 (1998), arXiv:hep-ph/9804212
[58] F. James, CERN Program Library Long Writeup D506, Version 94.1 (CERN Geneva, Switzerland)
[59] K. Golec-Biernat and M. Wusthoff, Phys. Rev. D **59**, 014017 (1998), arXiv:hep-ph/9807513
[60] R. Baier *et al*., Phys. Lett. B **539**, 46 (2002), arXiv:hep-ph/0204211
[61] H. Kowalski, T. Lappi and R. Venugopalan, Phys. Rev. Lett. **100**, 022303 (2008), arXiv:0705.3047
[62] J. L. Albacete and C. Marquetb, Prog. Part. Nucl. Phys. **76**, 1 (2014), arXiv:1401.4866
[63] F. Arleo and C. Naïm, JHEP **07**, 220 (2020), arXiv:2004.07188
[64] P. Ru *et al*., Phys. Rev. D **103**, L031901 (2021), arXiv:1907.11808
[65] R. Aaij *et al*. (LHCb Collaboration), Phys. Lett. B **774**, 159-178 (2017), arXiv:1706.07122
[66] S. Acharya *et al*. (ALICE Collaboration), Phys. Lett. B **827**, 136943 (2022), arXiv:2104.03116
[67] P. Duwentäster *et al*., Phys. Rev. D **104**, 094005 (2021), arXiv:2105.09873
[68] S. Kumano, AIP Conf. Proc. **1056**, 444 (2008), arXiv:0807.4207
[69] A. Bursche *et al*., Technical Report LHCb-PUB-2018-015, CERN-LHCb-PUB-2018-015 (2018)